Simulation of Resonant Tunneling Diodes Using ATLAS

Abstract

This article describes a model for Resonant Tunneling Diodes (RTDs) implemented within ATLAS framework. The model is based on a self-consistent solution of Poisson and Non-Equilibrium Green's Function (NEGF) equations with an effective mass Hamiltonian. Simulation results are presented for generic GaAs and SiGe RTDs.

Introduction

Resonant tunneling diodes (RTD) exhibit I-V characteristics with a negative differential resistance (NDR) region. This property finds numerous applications in ultra-fast circuits, amplifiers, oscillators, frequency converters, etc. The physics of NDR region is based on quantum electron tunneling from the emitter to the energy level in the central well of the double barrier structure and further to the collector: when the energy level in the central well is pulled below the emitter energy, the tunneling current vanishes. When modeling RTDs, a significant challenge lies not only quantum transport, but also in finding and resolving extremely narrow states in the central well and quasi-bound states in the emitter, which is required for treating electrostatic effects correctly. In this article we describe how these issues have been addressed in ATLAS and show simulation results for typical n-type GaAs and p-type SiGe resonant tunneling diodes.

Methodology

The model is based on a solution of 1D Non-equilibrium Greens Function (NEGF) equations, solved self-consistently with Poisson equation. No transport in perpendicular direction is allowed. We assume a multiple band effective mass band structure. The conduction and valence bands are parabolic and isotropic in the perpendicular plane, which allows us to perform integration of carrier and current densities over the k-space analytically.

In order to launch the model, specify N.NEGF_PL and/or P.NEGF_PL on the MODELS statement. The 2D device is split into 1D slices, treated independently. In each slice a 1D transport equation will be solved. Current densities are integrated over all slices in order to obtain total current through the device. If all slices along transport direction are equivalent, a simpler version of the model can be launched by N.NEGF_PL1D and/or P.NEGF_PL1D, which would copy carrier density from the first slice to all other slices. Orientation of the 1D carrier transport is given by SP.GEOM=1DX or 1DY(default) parameter on the MODELS statement.

The model assumes that the emitter and collector regions are in quasi-equilibrium, i.e. the resistance of this regions is much smaller that that of the central double barrier structure. This is done by assigning these regions the EQUIL.NEGF parameter on the REGION or MODELS statement. The equilibrium regions are further assigned a broadening parameter (so called "optical potential"), which is a small imaginary number added to the onsite potential of the Hamiltonian and is required to fill emitter quasi-bound states. Normally, these states are filed with electrons scattered by inelastic phonons. However, we avoid including inelastic phonon scattering because it would make the model too computationally intensive. The broadening is set by the ETA.NEGF parameter on the MODELS statement, with a default of 6.6 meV. The broadening is given an exponential decay at energies below the band edge, with a characteristic tail of kT/20.

ATLAS solves NEGF transport equations on a highly non-uniform energy grid, with the size set the ESIZE.NEGF parameter on the MODELS statement. It is of absolute importance to construct the energy grid, which would resolve all resonant peaks in the transmission, current spectrum and density of states, because these quantities determine total current and carrier density profile. The creation of energy grid is done by solving for eigen energies in the whole device using Quantum Transmitting Boundary Method (QTBM). In this method, open boundary conditions in the contacts are explicitly included into the Hamiltonian, thus making the eigen problem non Hermitian and non linear. Real and imaginary parts of the eigen energies allow one to predict the position and the width of the resonant peaks and to place a sufficient number of energy grid points in the important energy regions. See references [1] and [2] for the details of the QTBM method and energy grid construction.

After solving NEGF equations, ATLAS computes carrier density, I-V characteristics and energy dependent quantities such as transmission, DOS, carrier density spectrum and current density spectrum. In order to look at the energy dependent quantities, use PROBE statements and specify location and band of the quantity. Additionally, it is possible to compute and store eigen energies and wave functions using QTBM method as a post-processing. This is done with parameter NEGF.EIG on SAVE or SOLVE statements. The PROBE statement can also be used to track the value of some quantities with bias and log them into the I-V file.

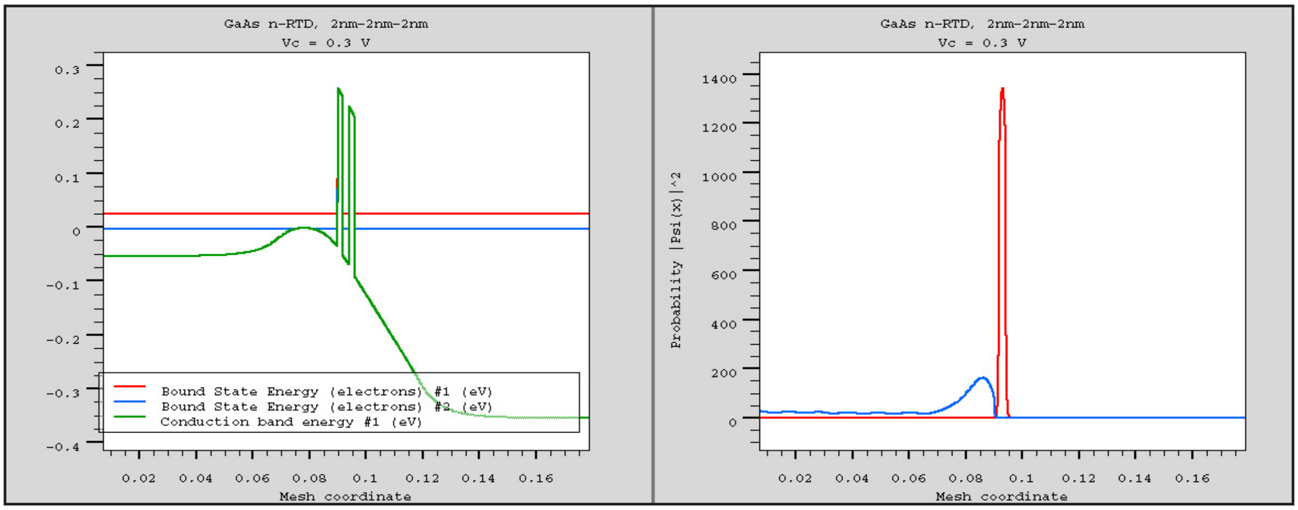

Figure 1. (Left panel) Conduction band profile at a bias of 0.3V. The horizontal lines show the eigen energiers in the emitter (blue) and in the well (red). (Right panel) Probability functions, corresponding to the bound states in the emitter (blue) and the well (red).

Simulation Results

a. GaAs n-RTD

As a first example, we consider a GaAs n-type RTD. It has a double barrier structure with 2 nm wide barriers and 2 nm wide well. The emitter and collector regions are doped to 10^{18} cm^{-3}, while the central region with the double barrier structure is left intrinsic.

The conduction band profile at applied bias of 0.3 V is shown in Figure 1 (left panel) together with energies corresponding to the lowest eigen states in the emitter (blue) and the well (red). At low voltages, the resonant energy in the well (red) is much higher energetically than the energy of emitter states. The right panel of Figure 1 shows the corresponding probability functions (square of absolute value of wave function). The resonant state is perfectly localized in the well, with almost no leakage outside of the barriers. The probability function of the emitter quasi-bound state is localized in front the barrier, but also shows a significant tail due to leakage into the emitter.

The eigen energy in the well is important because it is at this energy that electrons pass through the structure. This can be seen on the spectra of transmission probability and current density (Figure 2, left). Both transmission and current spectra show a sharp narrow peak at the resonant energy. The total current through the device will be given by the integral over the whole current density spectrum, with the resonant peak being the main contribution. Also shown is the energy resolved local density of states (DOS) in the well and emitter potential. The large broadening of the emitter DOS is the consequence of leakage into the rest of the contact, while the extreme narrowness of the DOS in the well is due to strong localization of the well state. Total carrier density will depend on the integral over local DOS spectra. Thus, the correct treatment of electrostatic effects will depend on proper resolution of the resonant peaks in the local DOS.

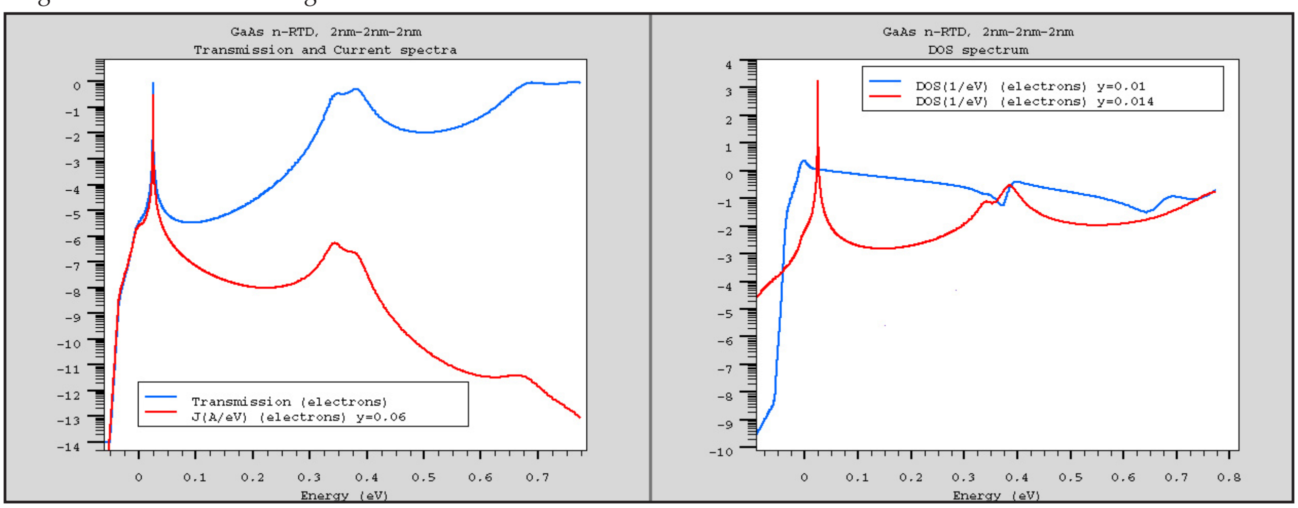

Figure 2. (Left panel) Spectrum of transmission (blue) and current density (red) at a bias of 0.3 V. (Right panel) Spectrum of the local density of states in the emitter(blue) and the well (red).

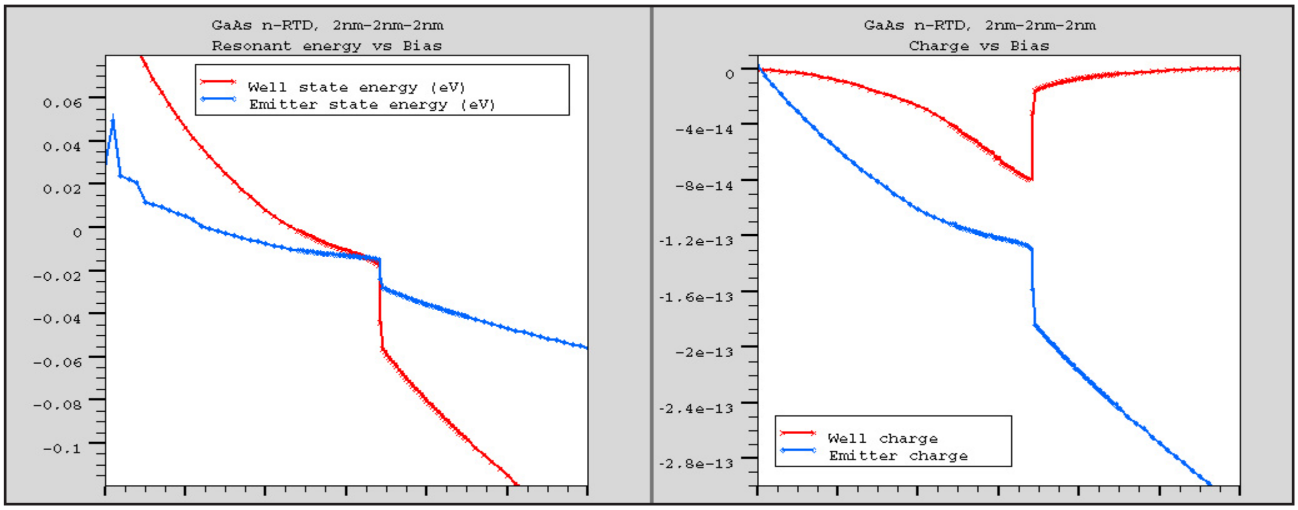

Figure 3. (Left panel) Dependence of the eigen energies in the emitter (blue) and the well (red) on applied bias. (Right panel) Total charge in the emitter (blue) and the well (red).

As bias increases, the resonant energy of the well is pulled down to lower energies, where more and more carriers can pass through the device and hence the current and the charge in the well grow. On Figure 3 we used PROBE statements to track the energies the two states with bias (left panel) and total charge in the well and emitter. The well energy is more responsive to bias and eventually decreases below the emitter quasi-bound state. When this happens, the supply of carriers to the well is cut off. By virtue of electrostatics, the lack of electrons is compensated by a sudden fall of the conduction band and all other related quantities. As seen from the right panel of Figure 3, the electron charge in the well cannot be recovered even after the fall. Instead, the electron charge in the emitter increases to ensure the charge neutrality.

The decrease of the resonant energy below the emitter state energy, leads to the slight saturation over a short bias range (Figure 4). It then followed by the sharp NDR region on the I-V characteristics, corresponding to the fall of the well resonant energy at the threshold bias of 0.68 V. Further increase of the bias leads to the decrease of contribution to the current by low energy carriers and simultaneous increase of the contribution due to electrons flying over the barrier.

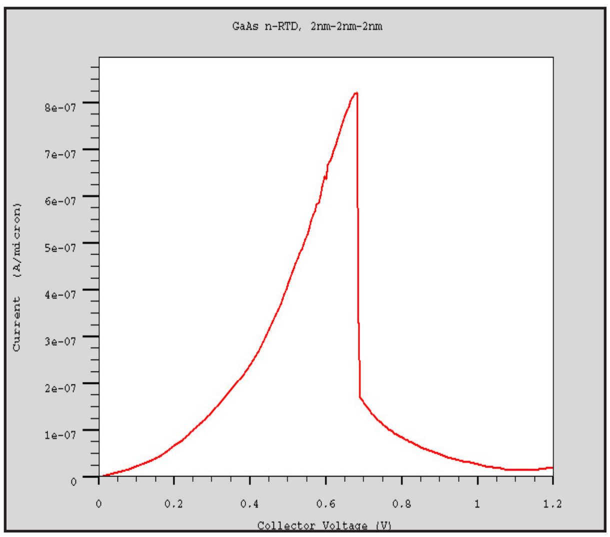

Figure 4. Current-voltage characteristics of n-type GaAs RTD.

The electrostatic charging of the central well is also demonstrated on the Figure 5, where carrier density profile is shown at biases of 0.1, 0.3, 0.6 and 0.7 V. The charge in the well grows until the threshold bias is reached. Above the threshold, the well charge is transferred to the emitter.

b. SiGe p-RTD

Let us now briefly look at the simulation results for p-type SiGe RTD with Si barriers. The barriers are 2nm wide Si layers separated by a 2nm well. We employ a two-band model for holes. The material parameters can be set on the MATERIAL statement using parameters MHH, MLH for effective masses and DEV.HH and DEV.LH for band off-sets. The hole effective masses were taken with following values: mhh(SiGe)=0.426, mlh(SiGe)=0.1132 and mhh(Si)=0.49 , mlh(Si)=0.16. The valence band off-sets in SiGe are 0.32 eV for heavy holes and 0.26 eV for light holes. We can see on Figure 6, that light holes, in addition to lower mass, also have lower confinement barriers. Both these factors make their confinement in the well less perfect. This is seen as a tail of the light hole wave function leaking out of the well. The consequence of the poor confinement is a large broadening of light holes resonant states and hence a less pronounced NDR region.

This is demonstrated on Figure 7, where we plot transmission probability for each band. The full width at half maximum of the first peak in transmission is estimated at 0.2 meV for heavy holes (red) and 20 meV for light holes (blue). We can also see that the transmission peak for light

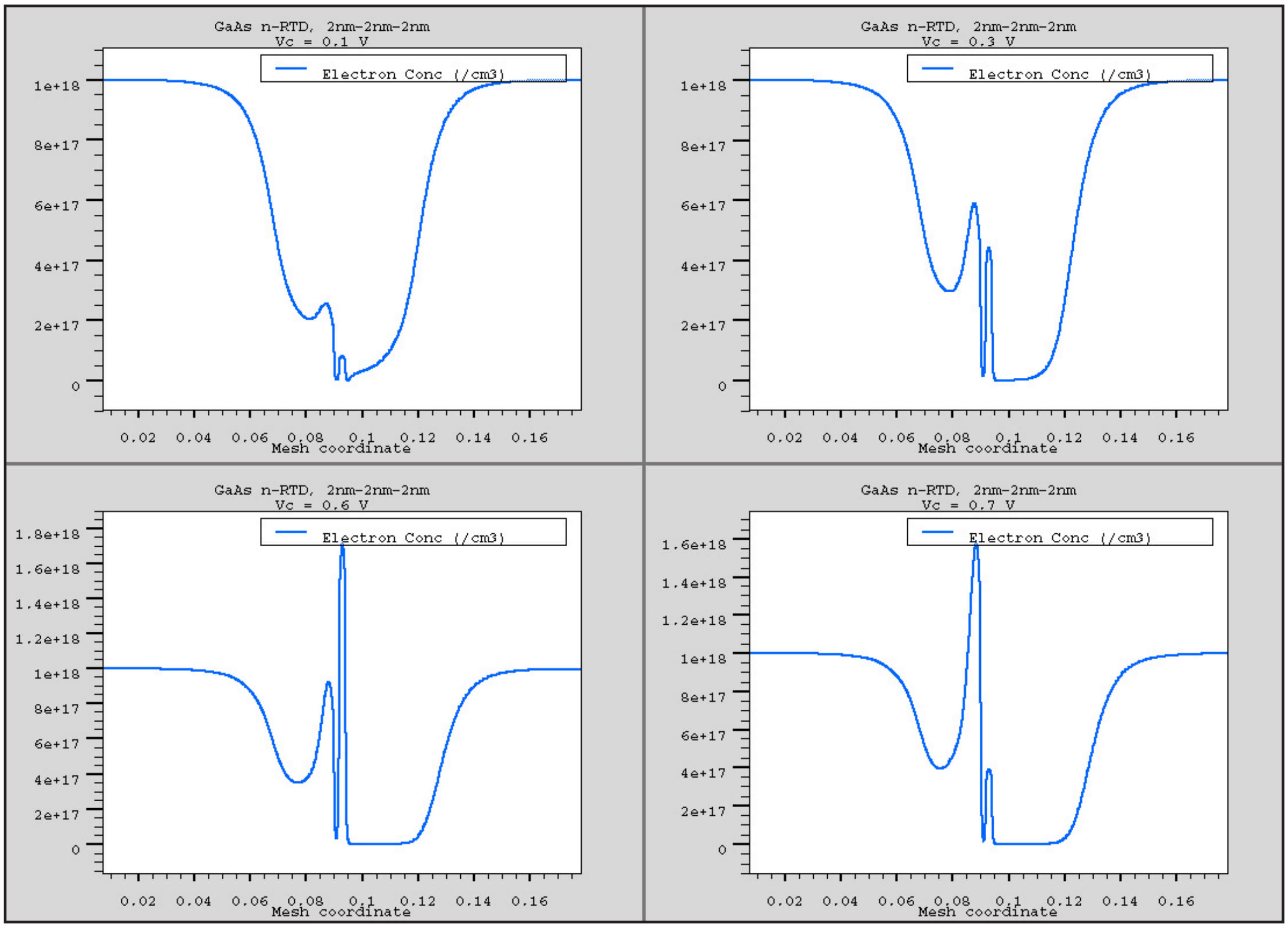

Figure 5. Electron density profiles at biases of 0.1, 0.3, 0.6 and 0.7 V. Note the non-monotonic behavior of the charge in the well.

holes is quite close to the emitter Fermi level, which gives a significant contribution to the total current. Even if the heavy holes are cut off at higher bias, the light holes will continue to conduct, resulting in a large valley current.

Finally, on Figure 8 we show the I-V characteristics of the SiGe p-RTD. As expected from the previous discussion, the first NDR region due to the heavy holes is not pronounced due to a large valley current, contributed by the light holes. The second NDR region due to light holes is much smoother, because of the large broadening of the transmission peak. The valley current is again high due to a presence of the second heavy hole transmission peak.

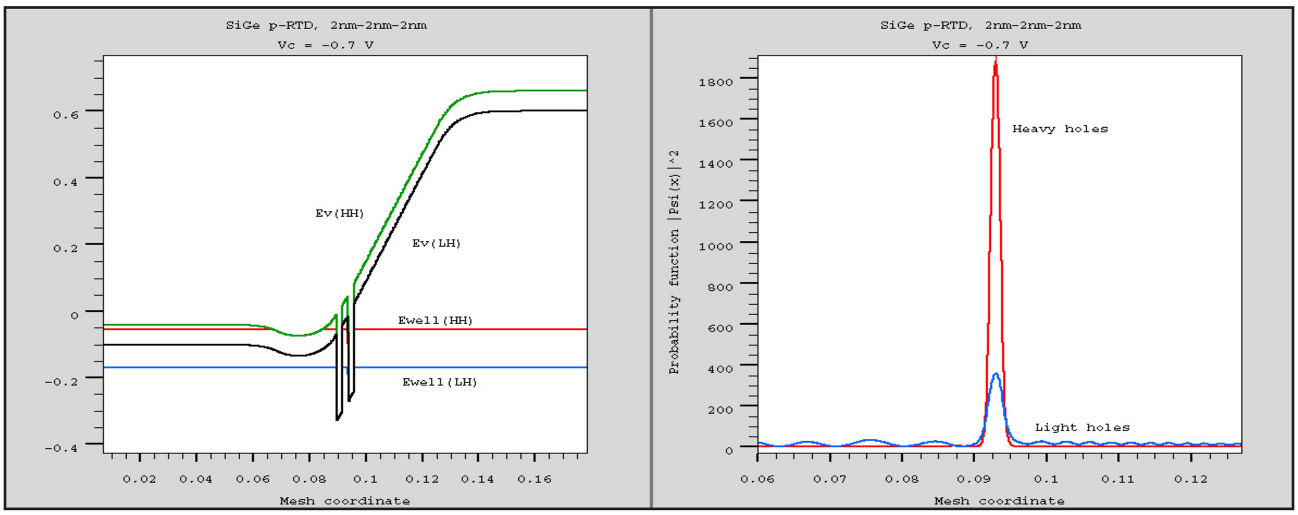

Figure 6. (Left panel) Valence band profile for heavy and light hole bands. Horizontal lines show highest bound state energies for the two bands. (Right panel) Probability function for the heavy and light hole states confined in the well.

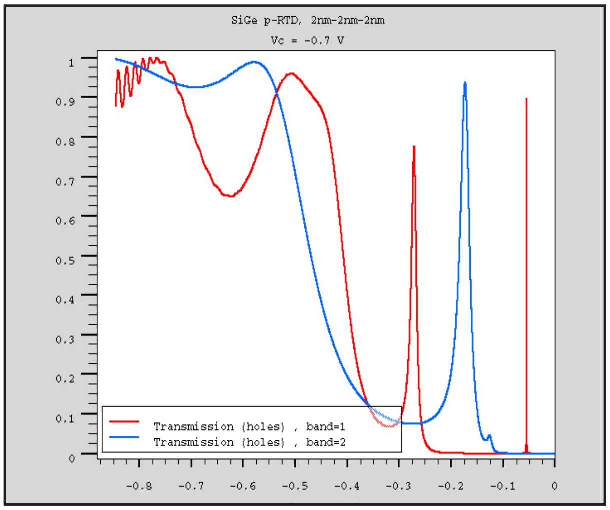

Figure 7. Transmission probability for heavy (red) and light (blue) holes.

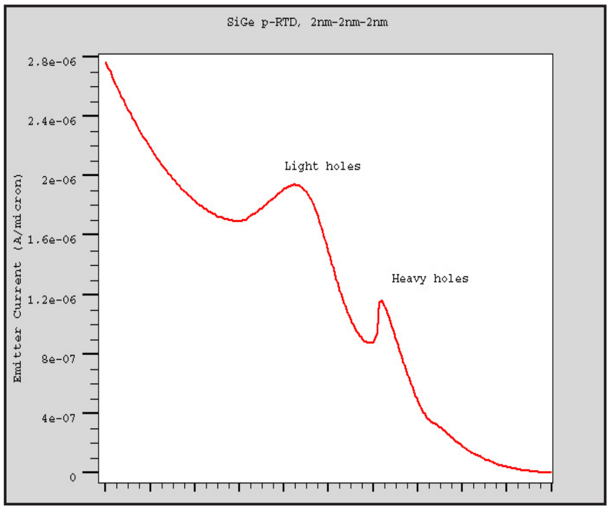

Figure 8. Current voltage characteristics of the SiGe p-type RTD. Multiple NDR regions correspond to different hole bands.

Conclusion

We presented a model for resonant tunneling diodes, based on Non Equilibrium Greens function approach. The model allows treating planar devices with arbitrary materials using a multiple band effective mass Hamiltonian. The model has simplicity of a 1D case but provides reach information on the position of resonant levels, wave functions and transmission probabilities and the I-V characteristics, which ultimately give insight into physics of the device operation.

By comparing our result for n- and p-type RTDs, we conclude that in order to get a pronounced NDR region, a number of material requirements should be met. Among them are the absence of other bands, which can create additional conducting channels and high enough effective mass of the well for better confinement. The latter requirement is opposite to the need for high enough confinement energy, required for higher threshold voltage. Computational modeling using ATLAS can provide an important insight to make required design trade-offs.

References:

1. C. L. Fernando and W. R. Frensley, “An efficient method for the numerical evaluation of resonant states”, J. Appl. Phys., 76, pp. 2881-2885.
2. G. Klimeck, R. K. Lake, R. C. Bowen, C. L. Fernando and W. R. Frensley, “Resolution of Resonances in a General Purpose Quantum Device Simulator (NEMO)”, VLSI Design, 6, pp. 107-110.